Improving Parenchyma Segmentation by Simultaneous Estimation of Tissue Property T_1 Map and Group-Wise Registration of Inversion Recovery MR Breast Images

Ye Xing[1], Zhong Xue[2], Sarah Englander[2], Mitchell Schnall[2], and Dinggang Shen[2,3]

[1] Dept of Bioengineering
[2] Dept of Radiology, University of Pennsylvania, PA 19104
{Ye.Xing,Sarah.Englander,Mitchell.Schnall}@uphs.upenn.edu,
zxue@tmhs.org
[3] Dept of Radiology and Biomedical Research Imaging Center, University of North Carolina, Chapel Hill, NC 27599
dgshen@med.unc.edu

Abstract. The parenchyma tissue in the breast has a strong relation with predictive biomarkers of breast cancer. To better segment parenchyma, we perform segmentation on estimated tissue property T_1 map. To improve the estimation of tissue property (T_1) which is the basis for parenchyma segmentation, we present an integrated algorithm for simultaneous T_1 map estimation, T_1 map based parenchyma segmentation and group-wise registration on series of inversion recovery magnetic resonance (MR) breast images. The advantage of using this integrated algorithm is that the simultaneous T_1 map estimation (E-step) and group-wise registration (R-step) could benefit each other and jointly improve parenchyma segmentation. In particular, in E-step, T_1 map based segmentation could help perform an edge-preserving smoothing on the tentatively estimated noisy T_1 map, and could also help provide tissue probability maps to be robustly registered in R-step. Meanwhile, the improved estimation of T_1 map could help segment parenchyma in a more accurate way. In R-step, for robust registration, the group-wise registration is performed on the tissue probability maps produced in E-step, rather than the original inversion recovery MR images, since tissue probability maps are the intrinsic tissue property which is invariant to the use of different imaging parameters. The better alignment of images achieved in R-step can help improve T_1 map estimation and indirectly the T_1 map based parenchyma segmentation. By iteratively performing E-step and R-step, we can simultaneously obtain better results for T_1 map estimation, T_1 map based segmentation, group-wise registration, and finally parenchyma segmentation.

1 Introduction

Breast cancer is the most common cancer in women. Breast cancer surveillance is improved through accurate assessment of the risk to develop cancer, which can be carried out by studying certain predictive biomarkers. Mammogram breast density has been demonstrated to be a biomarker of breast cancer risk [1]. The proposed MRI based predictive biomarkers are parenchyma volume and parenchyma enhancement

D. Metaxas et al. (Eds.): MICCAI 2008, Part I, LNCS 5241, pp. 342–350, 2008.

pattern. Parenchyma volume should represent a more precise anatomic measure than mammogram density, while parenchyma enhancement intensity should correlate with an active proliferation and thus a risk of cancer [2]. Therefore, to diagnose breast cancer early and prevent morbidity and mortality, the quantitative analysis of these predictive biomarkers in parenchyma is desired. As a basis to analyze the proposed MRI based biomarkers, it is essential to accurately segment parenchyma, one of the two main breast tissues, from breast.

So far, there are mainly two types of methods proposed for segmenting parenchyma tissue from breast MR images, i.e., intensity-based segmentation and tissue property based segmentation. Intensity-based segmentation differentiates tissues from their intensities and has its own drawbacks in images with intensity inhomogeneity. Tissue property based segmentation uses MR physics to characterize the intrinsic properties of tissue, which is believed to be more robust to intensity inhomogeneity. T_1 value based parenchyma segmentation belongs to this category, which utilizes the intrinsic physical fact that parenchyma and fat have different T_1 values [3]. To develop T_1 value based parenchyma segmentation, the accurate estimation of T_1 value for each pixel in the image is an extremely important step. Our paper focuses on how to improve T_1 map estimation for achieving a better segmentation of parenchyma.

To estimate T_1 value, our group uses a 3D inversion recovery spoiled gradient echo sequence to collect series of inversion recovery images with T_i varying from 0.2 second to 1.6 seconds, and T_1 value is estimated by fitting the intensities of these inversion recovery images to the solution of Bloch equation. There are two main problems in T_1 estimation, and both of them decrease the accuracy of T_1 estimation:

1) The estimated T_1 is rather noisy due to the complexity of the non-linear equations to be fitted;
2) The estimated T_1 is inaccurate due to body motions during the imaging acquisition.

Accordingly, we here present a novel framework of joint T_1 map *estimation*, T_1 map based parenchyma *segmentation* and group-wise *registration* of inversion recovery images. It has its merit in solving T_1 map estimation, tissue segmentation, and image registration simultaneously, thus eventually improving parenchyma segmentation. In particular, parenchyma segmentation based on the estimated T_1 map could reduce the noise in T_1 map estimation by using an edge-preserving smoothing, and could produce tissue probability maps to guide the group-wise registration for more robust registration. Meanwhile, group-wise registration based on the previously produced probability maps could compensate the effect of body motions and thus improve T_1 estimation and parenchyma segmentation. By iteratively repeating these steps, we could improve T_1 estimation and finally parenchyma segmentation, which is important for quantitative analysis of predictive biomarkers of breast cancer.

2 Method

In the following, T_1 map estimation and T_1 map based parenchyma segmentation, as well as group-wise registration of probability maps, are described in Subsections 2.1 and 2.2, respectively.

2.1 T_1 Map Estimation and T_1 Map Based Parenchyma Segmentation

Our novel parenchyma segmentation is based on intrinsic tissue parameter T_1, which is more robust to intensity inhomogeneity. To get better segmentation results, the accuracy of T_1 estimation is important. In this step of T_1 map estimation and T_1 map based parenchyma segmentation: T_1 map *estimation* provides a basis for segmentation. Meanwhile, *segmentation* based on T_1 map not only provide the parenchyma segmentation results to guide group-wise registration (with details in Subsection 2.2), but also help perform a same-tissue-type-smoothing on previous estimated noisy T_1 map, which would eventually improves parenchyma segmentation.

2.1.1 T_1 Map Estimation

The image data were acquired using a 3D inversion recovery spoiled gradient echo sequence [4]. For each breast, five series of 3D images, $\{I^m, m=1,\ldots,5\}$, were acquired by using five different sets of inversion time T_i and repetition time T_R, i.e., $\{(T_i^m, T_R^m), m=1,\ldots,5\}=\{(1600, 280), (800, 280), (400, 280), (200, 280), (140, 280)\}$ in a unit of *ms*. The observation flip angle is fixed to $\alpha=20^0$ during all data acquisition. It takes 10-15 minutes to acquire 5 series of 56*256*256 inversion recovery (IR) images.

The intensities in each acquired image I^m can be theoretically represented by a solution of Bloch equation as defined next. Given T_i^m, T_R^m, and α for each image I^m, the theoretical intensity at each voxel v is $\hat{I}^m(v)$, which is a function of three position-dependent parameters, i.e., T_1 value $T_1(v)$, equilibrium magnetization $S_0(v)$, and inversion pulse flip angle $\beta(v)$. Notice that $T_1(v)$ is tissue-dependent, while two parameters $S_0(v)$ and $\beta(v)$ are generally tissue-independent. The relationship among these parameters is mathematically defined as follows:

$$\hat{I}^m(v)\Big|_{T_1(v),S_0(v),\beta(v)} = S_0(v)\left(1-\exp\left(-\frac{T_i^m}{T_1(v)}\right)\right)+\frac{S_0(v)\left(1-\exp\left(-\frac{T_R^m}{T_1(v)}\right)\right)\exp\left(-\frac{T_i^m}{T_1(v)}\right)\cos(\beta(v))}{1-\exp\left(-\frac{T_R^m}{T_1(v)}\right)\cos(\alpha)}. \quad (1)$$

This equation indicates that three parameters $T_1(v)$, $S_0(v)$, and $\beta(v)$ on each voxel v can be estimated from five acquired intensities, $\{I^m(v), m=1,\ldots,5\}$, by minimizing the fitting errors as defined in equation (2) below. This equation requires that the theoretically estimated intensities $\hat{I}^m(v)$ should best fit with the practically acquired intensities $I^m(v)$ on each voxel v, e.g.,

$$E_{estimation} = \sum_v \sum_{m=1}^{M} \left(I^m(v) - \hat{I}^m(v)\Big|_{T_1(v),S_0(v),\beta(v)}\right)^2, \quad (2)$$

where $M=5$ in our study. A gradient-based optimization algorithm can be used to search for suboptimal solutions, based on the initializations provided for $T_1(v)$, $S_0(v)$, and $\beta(v)$. As indicated above, random values will be provided in the first iteration of T_1 map estimation, while in other iterations the previously estimated T_1 map after edge-preserving smoothing will be used as an initialization for new T_1 map estimation.

2.1.2 T_1 Map Based Parenchyma Segmentation

Improving parenchyma segmentation based on T_1 map is our final goal, which could result in a potentially important breast cancer risk biomarker. Besides, the tentative segmentation results produced during the T_1 map estimation procedure can also help to perform an edge-preserving smoothing for the iteratively estimated noisy T_1 map. In particular, Fuzzy C-means is used for parenchyma segmentation [5].

In T_1 map estimation, the energy function $E_{estimation}$ in Eq. (2) can be very complex, thus the estimated T_1 map can be noisy due to the lack of spatial smoothness constraints on estimated T_1 map. To avoid this, we perform a T_1 map based parenchyma segmentation to determine tissue class by which an edge-preserving smoothing filter is built to smooth T_1 values only for the voxels with the same tissue class. Meanwhile, the improved T_1 map estimation helps produce more accurate and less noisy parenchyma segmentation. By iteratively repeating these steps, we can achieve both better estimation and segmentation of T_1 map. Also, with the segmentation results, tissue probability maps would be built for group-wise registration, as detailed in Section 2.2.1 below.

2.2 Group-Wise Registration

As mentioned above, registration among different time images is necessary to compensate for the patient's motion during image acquisition, and can benefit for the T_1 map estimation, T_1 map based parenchyma segmentation, and eventually parenchyma segmentation. We will use group-wise registration method to align all different time images simultaneously, rather than using pair-wise registration methods which can potentially produce bias due to the selection of template [6].

Generally, group-wise image registration is based on the similarity of image intensities, e.g., using correlation coefficient and mutual information. For our application, we first calculate the tissue probability map in each time point image, and the registration of different time point images is based on the respective tissue probability maps. This is because, based on physiological fact, the tissue probability is a consistent factor and the same tissue should have similar probability in different time point images.

Before giving the details of our proposed group-wise registration method, we first define $I^{virtual}$ as a virtual image where all collected images $\{I^m, m=1,\ldots,5\}$ will be registered. The transformation from the m-th inversion recovery image to the virtual image $I^{virtual}$ is defined as $h^m(v)$, where $v=1,\ldots,N$ is a voxel in the image space. $\boldsymbol{H}^m=\{h^m(v), v=1,\ldots,N, m=1,\ldots,5\}$ represents all estimated transformations for all inversion recovery images. The segmentation result in $I^{virtual}$ is defined as $\boldsymbol{S}=\{S(v), v=1,\ldots,N\}$, where $S(v)$ denotes the segmentation result for a pixel v in $I^{virtual}$.

2.2.1 Tissue Probability Map

The tissue probability map in each time image $I^m(v)$ can be estimated with the help of T_1 map segmentation result $S(v)$ in the space of virtual image $I^{virtual}$. Assume for each image $I^m(v)$, all pixels with the same tissue label c, i.e., $S(v)=c$, form a Gaussian distribution. This way, we can obtain a probability map for each image in $\boldsymbol{I}=\{I^m(v), m=1,\ldots,5\}$, e.g., $\boldsymbol{P}=\{P^m(v,c), m=1,\ldots,5, c \text{ is a tissue label}\}$. Here, $P^m(v,c)$ is the tissue probability of $I^m(v)$ belonging to a tissue class c, which can be defined as:

$$P^m(v,c) = P^m\left(I^m(v) \mid S(v)=c\right) = \frac{1}{\sqrt{2\pi\sigma_{m,c}}} \exp^{-\frac{\left(I^m(v)-\mu_{m,c}\right)^2}{2\sigma_{m,c}^2}}, \quad (3)$$

where $\sigma_{m,c}$, $\mu_{m,c}$ are the standard deviation and mean of image intensities, belonging to the tissue class c, in the image I^m (v). The average of all tissue probability maps $\boldsymbol{P}=\{P^m(v,c)\}$ is the virtual probability map $P^{virtual}$, where all individual probability maps should be registered during the group-wise registration.

2.2.2 Group-Wise Deformable Registration Using Tissue Probability Maps

Our group-wise registration on tissue probability maps is implemented using B-spline based image registration [7]. As mentioned, $\boldsymbol{H}^m=\{h^m(v),\ v=1,\ldots,N,\ m=1,\ldots,5\}$ is a transformation from individual tissue probability map P^m to the common virtual tissue map space $P^{virtual}$. The energy function that our group-wise registration will minimize is:

$$E_{reg} = \sum_{m=1}^{M}\sum_{i=1}^{N}\left(P^m\left(h^m(v),c\right) - P^{virtual}(v,c)\right)^2 \cdot \quad (4)$$

Based on the estimated transformation $\boldsymbol{H}^m$, we can align each inversion recovery image I^m to the common space as I'^m, (m=1,…,5), where I'^m is the aligned image of I^m.

2.3 Summary of Algorithm

Fig. 1 summarizes the overall framework of our proposed joint T_1 map estimation, T_1 map based parenchyma segmentation, and group-wise registration technique. It takes approximately 15-20 minutes to process 5 series of 56*256*256 IR images, by a Linux machine with 1.6GHz CPU and 8GB RAM.

Step (1): T_1 map estimation of inversion recovery images $\boldsymbol{I}=\{I^m\}$. Use random values as initialization for $T_1(v)$, $S_0(v)$ and $\beta(v)$, and then independently estimate their true values by minimizing the errors between the practically acquired intensities $I^m(v)$ and theoretically estimated intensities $\hat{I}^{m}(v)$ as detailed in Subsection 2.1.1.

Step (2): Segment the currently estimated T_1 map into two classes, i.e., parenchyma and fat, by using a tissue segmentation algorithm such as fuzzy segmentation algorithm [5].

Step (3): Perform an edge-preserving smoothing on the currently estimated T_1 map, therefore achieving a smoothed version of T_1 map. By repeating Step (2), we can obtain better tissue segmentation, and the corresponding voxels in $\boldsymbol{I}=\{I^m(v)\}$ has the same tissue label c.

Step (4): Calculate tissue probability maps $\boldsymbol{P}=\{P^m(v,c)\}$ of $\boldsymbol{I}=\{I^m\}$. Assume the intensities of a same tissue class c is distributed at a Gaussian way, and then the tissue probability for pixel v in the image I^m can be calculated as $P^m(I^m(v)|S(v)=c)$. (Details are in Subsection 2.2.1.)

Step (5): Compute an average probability map $P^{virtual}$ from $\boldsymbol{P}=\{P^m(v,c)\}$, where all individual probability maps $P^m(v,c)$ will be registered during the group-wise registration in Step (6).

Step (6): Group-wise registration of $\boldsymbol{P}=\{P^m(v,c)\}$ to the virtual average probability map $P^{virtual}$. The registration is implemented by B-spline based registration to minimize the differences between $P^m(v,c)$ and $P^{virtual}(v,c)$ as defined in Eq.(4).

Step (7): Generate the registered images $\{I'^m\}$, and check their differences with the corresponding results in the previous iteration. If total difference is smaller than a certain threshold, update $\boldsymbol{I}=\boldsymbol{I}'$, perform Steps (1)-(3) to obtain the final segmentation result and stop; otherwise, repeat Steps (1)-(7).

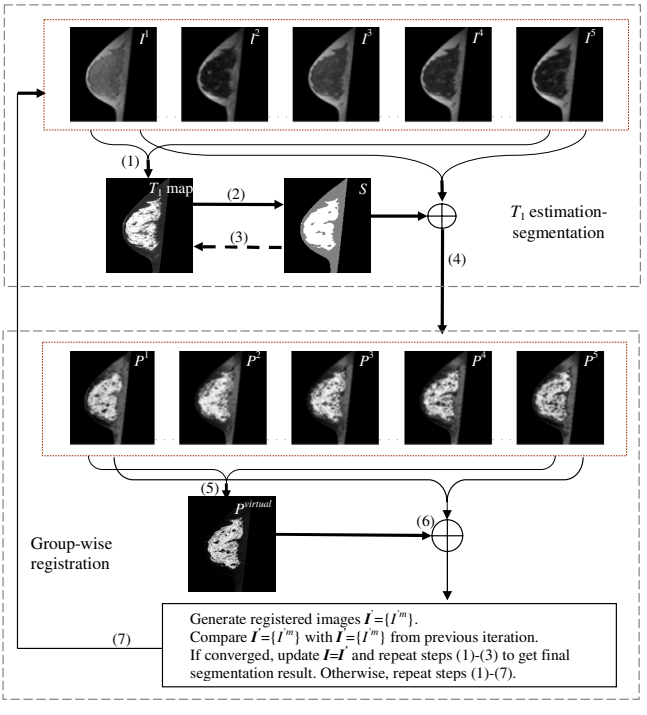

Fig. 1. The overall framework of joint T_1 map estimation, T_1 map based parenchyma segmentation and group-wise registration for MR breast inversion recovery images

3 Results

Experimental results are provided for demonstrating the performance of the proposed algorithm in joint T_1 map estimation, segmentation, and registration. *First*, the T_1 map estimation results are visually compared between the methods with and without using our joint framework of parenchyma segmentation and group-wise registration; validation of T_1 estimation on phantoms would also be presented. *Second*, quantitative comparisons on parenchyma segmentation are performed to show whether group-wise registration, rather than pair-wise registration, can improve the parenchyma segmentation.

3.1 Improvement of T_1 Map Estimation

We evaluated whether the use of joint T_1 map estimation, T_1 map based parenchyma segmentation and registration framework can effectively improve T_1 map estimation. Thus, in Fig. 2, we provide T_1 map estimation results, obtained by using or without using our joint framework. The maps in (b) and (a) represent, respectively, the T_1 maps estimated using our joint framework and without using our joint framework. For T_1 map in Fig. 2, the brighter pixels mean higher T_1 values, and they are more likely to be segmented as parenchyma in the breast tissue segmentation.

The difficulty of evaluating the improvement of T_1 map estimation is that the actual T_1 value of breast is not pre-known. One way to evaluate the accuracy of T_1 estimation is to evaluate the parenchyma segmentation results, as detailed in Subsection 3.2. The other way is to visually check the estimated T_1 values at the breast boundary where T_1 values should be lower, since there is no parenchyma at that region.

The red curves in (a), (b), and (c) are the selected regions of T_1 map for comparing the differences of T_1 values estimated. Inside red curves, the brighter pixels (with higher T_1 values) in (a) become darker in (b), which means that T_1 values in (b) are more accurately estimated since there is less parenchyma around the breast boundary. It can be better observed in the subtraction map (c). Also, the T_1 map in (b) is smoother than that in (a), which would improve the accuracy of parenchyma segmentation as demonstrated next. All of these show the better estimation of T_1 map with the proposed joint segmentation and registration framework.

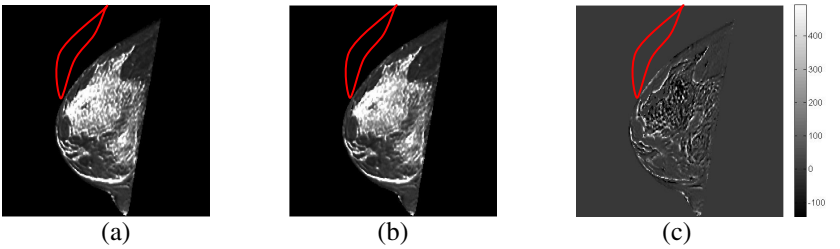

(a) (b) (c)

Fig. 2. T_1 map estimation results. (a) Estimated T_1 map without using joint parenchyma segmentation and group-wise registration. (b) Estimated T_1 map using joint parenchyma segmentation and group-wise registration. (c) Subtraction of (a) and (b).

We also performed a phantom test to validate the T_1 estimation. Phantoms containing six gadolinium-DTPA-BMA (Gd) saline solutions with different concentrations were studied. In practice, the relation of T_1 values between different Gd concentration solutions is modeled with a simple relationship as in Eq.(5):

$$\frac{1}{T_1(\rho_i)} - \frac{1}{T_1(\rho_0)} = \gamma \times (\rho_i - \rho_0), \tag{5}$$

where ρ_i (i=1,…,5) is Gd concentration and ρ_0 is the baseline of Gd concentration; γ is the relaxation rate of Gd; $T_1(\rho_i)$ is the mean estimated T_1 values for Gd concentration ρ_i and $T_1(\rho_0)$ is the mean estimated T_1 for baseline Gd concentration ρ_0.

The ground truth of relaxation rate for Gd is 4.04. The estimated relaxation rate by Eq.(5) using the estimated T_1 of each Gd concentration is 4.10, so the error rate is 1.5%. This test means that our method has the potential to provide accurate T_1 values between different tissues.

3.2 Validation of Parenchyma Segmentation Results

Parenchyma segmentation is validated by comparing automated segmentation results with manual segmentation results by radiologists. Note, by performing this comparison, we could indirectly evaluate the improvement of T_1 map estimation by the proposed method, since the parenchyma segmentation is based on T_1 map and thus its accuracy can reflect the accuracy of estimated T_1 map indirectly.

Table 1. Overlay percentage and volume error between automated segmentation (P) and manual segmentation (R). P1, P2, P3 are the automated segmentation results on three patients.

		P1 vs. R	P2 vs. R	P3 vs. R
Overlay percentage	w/o reg	85.5%	88.7%	89.9%
	w/ reg	**87.4%**	**90.2%**	**91.9%**
Volume error	w/o reg	16.0%	12.0%	10.6%
	w/ reg	**13.5%**	**10.3%**	**8.4%**

From Table 1, we could observe: *first*, our automated segmentation using estimated T_1 map has a great potential of segmenting parenchyma tissue as good as human raters, with the overlay percentage ($\frac{V_A \cap V_B}{(V_A+V_B)/2}$) around 87%-92% and volume error ($\frac{|V_A - V_B|}{(V_A+V_B)/2}$) around 10%, where V_A and V_B denote the segmentation results by automated or manual methods respectively; *second,* the algorithm with group-wise registration has a better segmentation results, compared to the algorithm without using group-wise registration, which shows the importance of using group-wise registration to align the inversion recovery images and to improve parenchyma segmentation and T_1 map estimation.

4 Conclusion

We have presented a joint T_1 map estimation, T_1 map based parenchyma segmentation, and group-wise registration framework for improving parenchyma segmentation from MR inversion recovery images. By using this joint framework, we can jointly solve the two main problems in T_1 map estimation which is essential for parenchyma segmentation, e.g., noises in the estimated T_1 map and body motions among inversion recovery images. Experimental results show the improved accuracy in parenchyma segmentation using our proposed joint framework. In the future, we will test the performance of our joint framework by more breast image data. Also, we will apply this developed method to several large breast cancer studies performed in our institute.

References

1. Brisson, J., Merletti, F., Sadowsky, N.L., Twaddle, J.A., Morrison, A.S., Cole, P.: Mammographic features of the breast and breast cancer risk. American Journal of Epidemiology 115, 428–437 (1982)
2. Hayton, P., Brady, M., Tarassenko, L., Moore, N.: Analysis of dynamic MR breast images using a model of contrast enhancement. Medical Image Analysis 1(3), 207–224 (1996)
3. Boston, R.C., Schnall, M.D., Englander, S.A., Landis, J.R., Moate, P.J.: Estimation of the content of fat and parenchyma in breast tissue using MRI T1 histograms and phantoms. Magnetic Resonance Imaging 23(4), 591–599 (2005)
4. Foo, T.K.F., Sawyer, A.M., Faulkner, W.H., Mills, D.G.: Inversion in the Steady State: Contrast Optimization and Reduced Imaging Time with Fast Three-dimensional Inversion-Recovery-prepared GRE Pulse Sequences. Radiology 191, 85–90 (1994)
5. Bezdek, J., Ehrlich, R., Full, W.: FCM: Fuzzy C-Means Clustering Algorithm. Computers & Geosciences 10(2-3), 191–203 (1984)
6. Bhatia, K.K., Hajnal, J.V., Puri, B.K., Edwards, A.D., Rueckert, D.: Consistent groupwise non-rigid registration for atlas construction. In: IEEE International Symposium on Biomedical Imaging: Nano to Macro, 2004, April 15-18 (2004)
7. Rueckert, D., Sonoda, L.I., Hayes, C., Hill, D.L.G., Leach, M.O., Hawkes, D.J.: Non-rigid registration using free-form deformations: Application to breast MR images. IEEE Transactions on Medical Imaging 18(8), 712–721 (1999)